Image Reconstruction of Subspace Object Using Electrical Resistance Tomography

Chang-Jin Boo, Ho-Chan Kim, Min-Jae Kang

School of Electrical & Electronic Engineering, Cheju National University

Abstract

Electrical resistance tomograpy (ERT) maps resistivity values of the soil subsurface and characterizes buried objects. The characterization includes location, size, and resistivity of buried objects. In this paper, truncated least squares (TLS) is presented for the solution of the ERT image reconstruction. Results of numerical experiments in ERT solved by the TLS approach is presented and compared to that obtained by the Gauss-Newton method.

Key Words : Electrical resistance tomography, Inverse problem, Nondestructive imaging, Gauss-Newton method, TLS method

1. Introduction

The definition of a ground electrode is "a conductor or group of conductors in intimate contact with the earth for the purpose of providing a connection with the soil". This definition does not refer to an actual ohm resistance value of the electrode. The resistance value is determined by the resistivity of soil with which these electrodes are in contact. As in the case of ground water, the current must pass through the soil to the assumed earth potential of $0\,\Omega$. When an object is grounded, it is then forced to assume the same zero potential as the earth. If the potential of the grounded object is higher or lower, current will pass through the grounding connection until the potential of the object and earth are the same. The earth electrode is that connection path from the equipment to the earth. The resistance of the electrode, measured in ohms, determines how quickly and at what potential energy is equalized. Hence, grounding is necessary to maintain an object's potential equal to that of the earth's [1].

The soil is the dynamic conductor for steady-state, natural, and man-made fault currents. Most soils naturally contain varying amounts of electrolytes that conduct electricity. As a result, the addition of moisture will enhance or reduce the conductive properties. In general, however, the greater the moisture contents in soil, the lower the resistivity. Temperature, like moisture, can have a significant impact on resistivity. Soil resistivity varies with temperature, especially when reaching 0 °C (the moisture in the soil freezes and the resistivity increases by almost three times its unfrozen value).

To determine the conductivity of the soil, a four-point ground meter is utilized. This test requires the user to place four equally spaced auxiliary probes into the earth to determine the actual soil resistance, traditionally in ohms-cm. This test must take place around the entire area to determine the soil value at all locations. This test is done at different spacing, 5 to 40 feet, to determine the resistance value at various depths. This knowledge will aid in the design and implementation of the correct ground system to meet the particular site requirements [2]. Soil values can range from 500 Ω cm with large amounts of electrolytes to over 1 million Ω cm in sandy dry soil.

Electrical Resistance Tomography (ERT) or, more generally electrical impedance tomography, is receiving an increasing interest from the scientific and industrial community aiming to develop a cheap and fast inspection tool for industrial applications [3]. Many applications of ERT have also been found in the geophysical field because the electrical resistivity is one of the most variables of physical properties in the subsurface [4]. The purpose of nondestructive ERT systems is to visualize internal regions of the object by means of external electrodes. Due to varying resistivities of internal materials, electric current passed through the object results in voltage changes measured on the surface. The performance of an ERT system can be stated in terms of spatial resolution of resistivity distribution, resistivity contrast and some other factors.

The majority of existing procedures for reconstructing resistivity distribution proved by electrical fields have been primarily based on linearized inversion techniques such as those used in diffraction or diffusion tomography. A general procedure to reconstruct the resistivity distribution consists of minimizing a quadratic cost function that emphasizes the sum of squared differences between measured and modeled data. Because in most cases the relationship between the property distribution function and the modeled data is nonlinear, the minimization is performed with a nonlinear search technique constructed by way of choosing a suitable number of iterations which eventually trace the road toward an extreme value of the cost function. The way this search is performed is usually a compromise between efficiency of the computations and stability of the method. A most common approach is referred to as the Gauss-Newton method, in which only first-order variations of the modeled data with respect to a variation in model parameters, the Jacobian or sensitivity matrix, is

computed at each iteration. Ill-conditioning, however, degrades the performance of the Gauss-Newton method for data contaminated with measurement error.

The sensitivity matrix is a complicated function of electric current, voltage and the unknown resistivity distribution. Improving the conditioning of the matrix by choosing a measurement method for the resistivity distribution is very difficult task since no explicit relationship can be seen. As an alternative, the regularization method is usually used to improve its conditioning [5]. The performance of the regularization method is closely related to the smoothing coefficient. A large coefficient distorts the information, while a small one has little effect.

In this paper, we present truncated least squares (TLS) approach for the ERT image reconstruction of subspace object. We begin our discussion with a review of finite element method (FEM) to solve 2D dc resistivity problems. The forward modeling is used for predicting apparent resistivities, which would be obtained on the surface of the sample. We then describe our inversion algorithm to analyze ERT measurements. Results of numerical experiments in ERT solved by the TLS approach is presented and compared to that obtained by the Gauss-Newton method. Finally, we discuss the performance of this approach through inverting synthetic data.

2. Image Reconstruction Using Electrical Resistance Tomography

The numerical algorithm used to convert the electrical measurements at the boundary to a resistivity distribution is described here. The algorithm consists of iteratively solving the forward problem and updating the resistivity distribution as dictated by the formulation of the inverse problem. The forward problem of ERT calculates boundary potentials with the given electrical resistivity distribution, and the inverse problem of ERT takes potential measurements at the boundary to update the resistivity distribution.

2.1 The forward problem

The application of FEM to a 2D dc resistivity problem is thoroughly discussed in Tang and Yang [6]. Its main advantage as compared with other numerical methods is that complicated geometries, general boundary conditions, and spatially variable or non-linear material properties can be handled relatively easily. Furthermore, it does not suffer from a singularity problem at the source point in resistivity modeling [7], as the source singularity is effectively smoothed out by minimizing an integral-formed functional. For completeness, the method is briefly outlined here. The partial differential equation governing the behavior of electric potential is described by Poisson's equation:

$$- \nabla \cdot \left(\frac{1}{\rho} \nabla u \right) = \nabla \cdot J_s \qquad (1)$$

where ρ is the electrical resistivity (Ωm), u is the poten-

tial (V), and J_s the impressed current source (A). The computation of the potential $u(x, y)$ for the given resistivity distribution $\rho(x, y)$ and boundary condition is called the forward problem. The numerical solution for the forward problem can be obtained using the FEM. In the FEM, the object area is discretized into small elements having a node at each corner. It is assumed that the resistivity distribution is constant within an element. The potential at each node is calculated by discretizing (1) into

$$K U_c = I_c \qquad (2)$$

where U_c is the vector of voltages at the FEM nodes and the electrodes, I_c the vector of injected current patterns and the matrix K is a functions of the unknown resistivities.

2.2 The inverse problem

The inverse problem, also known as the image reconstruction, consists in reconstructing the resistivity distribution $\rho(x, y)$ from potential differences measured on the boundary of the object. Ideally, knowing the potential on the whole boundary makes the correspondence between the resistivity distribution and the potential biunique. The relatively simple situation depicted so far does not hold exactly in the real world. The methods used for solving the ERT problem search for an approximate solution, i.e., for a resistivity distribution minimizing some sort of residual involving the measured and calculated potential values. From a mathematical point of view, the ERT inverse problem consists in finding the coordinates of a point in a M-dimensional hyperspace, where M is the number of discrete elements whose union constitutes the tomographic section under consideration. In the past, several ERT image reconstruction algorithms for the current injection method have been developed by various authors. To reconstruct the resistivity distribution inside the object, we have to solve the nonlinear ill-posed inverse problem. Regularization techniques are needed to weaken the ill-posedness and to obtain stable solutions.

A nonlinear inverse problem is generally solved by iteratively minimizing the discrepancy between data d and the model response $f(\rho)$, normalized by the standard deviations ε_i of the data

$$\Phi_d = \sum_i^n \left(\frac{d_i - f_i(\rho)}{\varepsilon_i} \right)^2 = \| (D(d - f(\rho)) \|_2^2 = \Phi_d^* \qquad (3)$$

where $D = \text{diag}(\varepsilon_i^{-1})$. Multi-dimensional problems are generally ill-posed considering data errors. Therefore, one has to introduce regularizing constraints like smoothness [8] or a-priori-information [9]. This can be accomplished by additionally minimizing a semi-norm $\| C(\rho - \rho_0) \|_2$, weighted by a regularization parameter λ

$$\Phi = \Phi_d + \lambda \Phi_\rho$$
$$= \| (D(d - f(\rho)) \|_2^2 + \lambda \| (C(\rho - \rho_0) \|_2^2 \qquad (4)$$

The matrix C represents the expectations to the model,

e.g., smoothness constraints. ρ_0 is the reference or a-priori model. The application of the Gauss-Newton method leads to an iterative scheme $\rho_{k+1} = \rho_k + \Delta\rho_k$ solving the regularized normal equations

$$((DS)^T DS + \lambda C^T C) \cdot \Delta\rho_k$$
$$= (DS)^T D(d - f(\rho_k)) - \lambda C^T C(\rho_k - \rho_0) \qquad (5)$$

Note that for a local regularization scheme effecting the model update $\Delta\rho$ instead of the model ρ the latter term vanishes. The Jacobian or sensitivity matrix S contains the partial derivatives of the model response with respect to the model parameters

$$S_{ij} = \frac{\partial f_i(\rho)}{\partial \rho_j} \qquad (6)$$

The Jacobian matrix $S \in R^{M \times N}$ is a full matrix, whereas the matrices $D \in R^{N \times N}$ and $C \in R^{M \times M}$ are generally sparse. The vectors have the dimensions $\rho \in R^M$ and $d, f \in R^N$. With $\mathcal{S} = DS$, the equation (5) can be written using generalized inverse matrices $\mathcal{S}^+$ and C^+

$$\Delta\rho_k = \mathcal{S}^+ D(d - f(\rho_k)) - C^+ C(\rho_k - \rho_0) \qquad (7)$$

where $\mathcal{S}^+ = (\mathcal{S}^T \mathcal{S} + \lambda C^T C)^{-1} \mathcal{S}^T$ and $C^+ = \lambda(\mathcal{S}^T \mathcal{S} + \lambda C^T C)^{-1}$. Furthermore, note that $\mathcal{S}^T \mathcal{S} + C^T C = I$.

The data are superposed by the response of the true model ρ_{true} and the noise n

$$d = f(\rho_{true}) + n \qquad (8)$$

Assuming in the kth iteration the model ρ_k is already close to the true model, a linearized Taylor expansion of $f(\rho_k)$ yields

$$d = f(\rho_k) + S(\rho_{true} - \rho_k) + n \qquad (9)$$

By insertion of $d - f(\rho_k)$ from equation (9) into equation (7), we obtain for $\rho_{est} = \rho_k$

$$\rho_{est} = \rho_k + \mathcal{S}^+ S(\rho_{true} - \rho_k) - C^+ C(\rho_k - \rho_0) + \mathcal{S}^+ Dn$$
$$= R^M \rho_{true} - (I - R^M)\rho_0 + \mathcal{S}^+ Dn \qquad (10)$$

The model estimate ρ_{est} is constructed by the true model and the starting model and contaminated by noise effects. The matrix $R^M = \mathcal{S}^+ \mathcal{S}$ combining the procedures of measurement and inversion is called resolution matrix. It serves as a kernel function transferring the reality into our model estimate and can be calculated using the generalized singular value decomposition [11]. Alternatively, the model resolution can be approximated by conjugate gradient techniques [12]. The operation of ERT algorithm is described in the flowchart of Fig. 1.
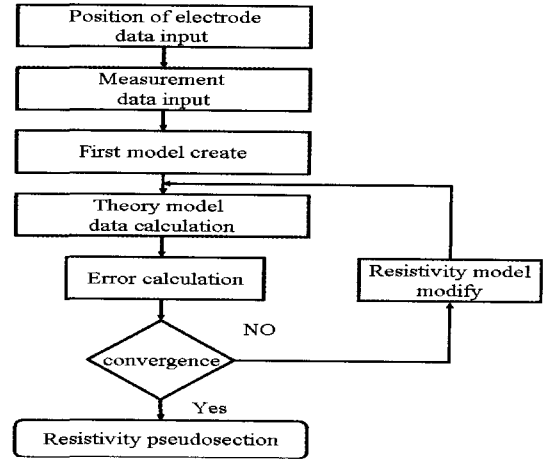

Fig. 1. Flowchart of ERT algorithm

2.3 The truncated least squares algorithm

In every iteration step k, the linearized subproblem (5) to be solved reads

$$((DS)^T DS + \lambda C^T C) \cdot \Delta\rho_k$$
$$= (DS)^T D(d - f(\rho_k))\{-\lambda C^T C(\rho_k - \rho_0)\}$$

Note that for local regularization schemes the term within $\{\ \}$ vanishes in the above equation. The solution $\Delta\rho_k$ depends on the matrices S, D, C and the vectors $\Delta d_k = d - f(\rho_k)$ and $\rho_k - \rho_0$. The equation can be interpreted as solution of $Ax = DS\Delta\rho_k = D\Delta d_k = b$ in a weighted least squares sense. In the following equation solvers are presented solving $Ax = b$ for x in least squares senses.

For small-scale systems the normal equations can be solved by matrix inversion of the left hand side matrix, which is always possible for $\lambda > 0$, by appropriate methods like Gaussian elimination or QR decomposition. In multidimensional inversion, the number of model parameter and data are quite large, which prohibits the use of direct inversion from both computer time and memory usage point of view. Hence, an approximate solution is sought using iterative methods.

The conjugate gradient method derived by Hestenes and Stiefel [12] is widely used for iteratively solving large-scale systems of equations $Ax = b$. Since in every iteration only one matrix vector product has to be calculated, it is primarily used for sparse A as arising in the discretization of partial differential equations. However, conjugate gradients are not restricted to sparse systems and can also be applied to the normal equations

Low-frequency components of the solution tend to converge faster than high-frequency parts in Krylov subspace methods. This can be used for an implicit regularization algorithm called truncated least squares (TLS) algorithm [13]. Assume a Marquardt type of regularization resulting in the damped normal equations

$$(A^T D^T DA + \lambda C^T C)x = A^T D^T Db\{-\lambda C^T C(\rho_k - \rho_0)\} \qquad (11)$$

Let z be the residual of the basis equation $z = D(Ax - b)$ and r denote the residual of the equation to be solved

$r = A^T D^T D(Ax - b) - \lambda C^T Cx = A^T z - \lambda C^T Cx$. Then, the solution of equation (11) is described in the following TLS algorithm.

The TLS algorithm

$k = 0$

$z_0 = D(Ax_0 - b)$

$p_0 = r_0 = A^T D^T z - \lambda C^T Cx_0$

while $k \leq k_{max}$ do

$q_{k+1} = DAp_k$

$\alpha_{k+1} = \dfrac{\| r_k \|^2}{q_k^T q_k^2 + \lambda p_k^T C^T Cp_k^2}$

$x_{k+1} = x_k + \alpha_{k+1} p_k$

$z_{k+1} = z_k - \alpha_{k+1} q_k$

$r_{k+1} = DAz_{k+1} - \lambda C^T Cx_{k+1}$

$\beta_{k+1} = \dfrac{\| r_{k+1} \|^2}{\| r_k \|^2}$

$p_{k+1} = r_{k+1} + \beta_{k+1} p_k$

$k = k + 1$

end while

3. Computer Simulation

The proposed TLS algorithm has been tested by comparing its results for numerical simulations with those obtained by Gauss-Newton method. Fig. 2 shows the synthetic model investigated in this paper. It is equally discretized in x from -1 to 42m and in y from 0 to 6m in block sizes of 1m×1m and consists of bodies with resistivities of 50 and 200 Ωm within a homogeneous background of 100 Ωm. Model parameters and data are the logarithms of the cell resistivities and the apparent resistivities, respectively. Table 1 shows the electrode arrangements investigated. A Wenner data set is simulated resulting in 273 single data.
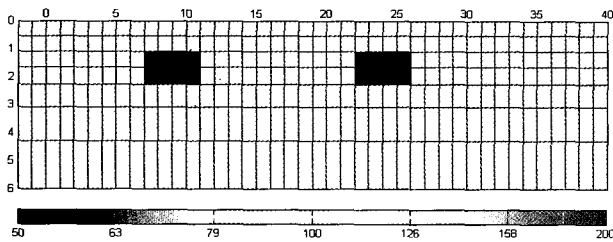

Fig. 2. Model parameterization and synthetic model consisting of two bodies of 50 Ωm or 200 Ωm in a homogeneous half-space of 100 Ωm.

Table 1. Definition of data sets

Variable	Value
Electode Arrangement	Wenner(CCPP)
Number of electrodes	41
Position of first electrode	-1 m
Electrode spacing	1 m
Separation n	6

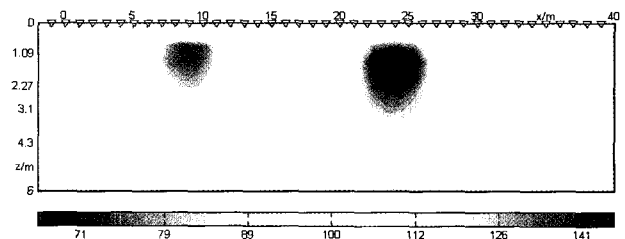For a Wenner data set, the TLS and two Gauss-Newton al-

gorithms are compared. Fig. 3 shows the inversion results of the numerical simulation for an assumed 3% noise data and a 1mV voltage resolution at 100mV current. The two Gauss-Newton schemes with fixed regularization ($\lambda = 30$) and L-curve produce noise artifacts from the third term of the right hand side of equation (10). The inversion result using TLS algorithm yields superior resolution quality and matches the synthetic model very well near boundaries.
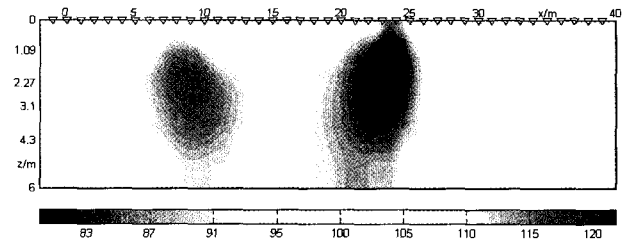
(a) Gauss Newton with fixed regularization
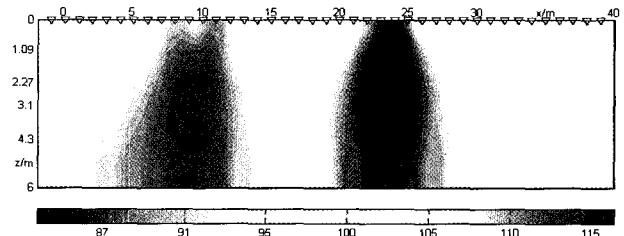
(b) Gauss Newton with L-curve

(c) Truncated LS

Fig. 3. Inversion results for TLS and two Gauss- Newton schemes using Wenner data set.

4. Conclusion

In this paper, an ERT image reconstruction method based on TLS approach was presented to improve the spatial resolution. A technique based on TLS algorithm was developed for the solution of the ERT inverse problem and superior result. The crucial point in nonlinear inversion is the choice of the regularization parameter, which strongly influences resolution properties and thus it has to be chosen carefully. Furthermore, the exploitation of a priori knowledge will produce very good reconstructions.

References

[1] J. Nahman and D. Salamon, "A practical method for the interpretation of earth resistivity data obtained from driven rod tests," IEEE Trans. Power Delivery, vol. 3, pp. 1375-1379, 1988.

[2] F. Dawalibi and C. J. Blattner, "Earth resistivity measurement interpretation techniques," IEEE Trans. Power App. Syst., vol. PAS-103, pp. 374-382, 1984.

[3] R. A. Williams and M. S. Beck, Process Tomography - Principles, techniques and application, Butterworth-Heinemann Ltd., 1995.

[4] P. Kearey and M. Brooks, An Introduction to Geophysical Exploration, 2nd Ed., Blackwell Scientific Pub., 1991.

[5] M. E. Kilmer and D. P. O'Leary, "Choosing regularization parameters in iterative methods for ill-posed problems," SIAM J. on Matrix Analysis and Applications, vol. 22, pp. 1204-1221, 2001.

[6] L. Tong and C. Yang, "Incorporation of tomography into two-dimensional resistivity inversion," Geophysics, vol. 55, no. 3, pp. 354-361, 1990.

[7] T. Lowry, M. B. Allen, and P. N. Shive, "Singularity removal: A refinement of resistivity modeling techniques," Geophysics, vol. 54, pp. 766-774, 1989.

[8] S. C. Constable, R. L. Parker, and C. G. Constable, "Occam's inversion: A practical algorithm for generating smooth models from electromagnetic sounding data," Geophysics, vol. 52, pp. 289-300, 1987.

[9] D. D. Jackson, "The use of a priori data to resolve non-uniqueness in linear inversion," Geophys. J. R. Astr. Soc., vol. 57, pp. 137-157, 1979.

[10] S. Friedel, "Resolution, stability and efficiency of resistivity tomography estimated from a generalized inverse approach," Geophys. J. Int., vol. 153, pp. 305 - 316, 2003.

[11] D. L. Alumbaugh and G. A. Newman, "Image appraisal for 2-d and 3-d electromagnetic inversion," Geophysics, vol. 65, no. 5, pp. 1455-1467, 2000.

[12] C. M. R. Hestenes and E. Stiefel, "Methods of conjugate gradients for solving linear systems," J. Res. Nat. Bur. Stand, vol. 49, pp. 409-436, 1952.

[13] L. R. Lines and S. Treitel, "Tutorial: A review of least square inversion and its application to geophysical problem," Geophysical Prospecting, vol. 32, pp. 159-186, 1984.

Chang-Jin Boo

He received his B.S. and M.S. degrees in Electrical Engineering from Cheju National University in 2001 and 2003, respectively. He is currently a Ph.D. student at Cheju National University.

Phone   : +82-64-754-3797
Fax   : +82-64-756-5281
E-mail   : boo1004@cheju.ac.kr

Ho-Chan Kim

He received the B.S., M.S., and Ph.D. degrees in Control & Instrumentation Engineering from Seoul National University in 1987, 1989, and 1994, respectively. He was a research staff from 1994 and 1995 at the Korea Institute of Science and Technology (KIST). Since 1995, he has been with the Department of Electrical Engineering at Cheju National University, where he is currently an associate professor.

Phone   : +82-64-754-3676
Fax   : +82-64-756-5281
E-mail   : hckim@cheju.ac.kr

Min-Jae Kang

He received the B.S. degree in Electrical Engineering from Seoul National University in 1982 and Ph.D degree in Electrical & Computer Engineering from University of Louisville in 1991. Since 1992, he has been with school of Electrical and Electronic Engineering at Cheju National University, where he is currently a professor.

Phone   : +82-64-754-3666
Fax   : +82-64-756-1745
E-mail   : minjk@cheju.ac.kr